# Synthesis, characterization, crystal structures, and superoxide dismutase activity of copper(II) octahedral complexes containing tri- and monodentate ligands

R. N. Patel[a]; K. K. Shukla[a]; Anurag Singh[a]; M. Choudhary[a]; D. K. Patel[a]

[a] Department of Chemistry, A.P.S. University, Rewa 486003, Madhya Pradesh, India

## PLEASE SCROLL DOWN FOR ARTICLE

# Synthesis, characterization, crystal structures, and superoxide dismutase activity of copper(II) octahedral complexes containing tri- and monodentate ligands

R.N. PATEL*, K.K. SHUKLA, ANURAG SINGH,
M. CHOUDHARY and D.K. PATEL

Department of Chemistry, A.P.S. University, Rewa 486003, Madhya Pradesh, India

Three new copper(II) complexes $[Cu(PSBP)_2](NO_3)(BF_4)$ (**1**), $[Cu(DAPBMA)_2](BF_4)_2$ (**2**), and $[Cu(ImH)_4(NO_3)_2]$ (**3**), where PSBP = 4-phenylsemicarbazide-2-benzoylpyridine, DAPBMA = 2,6-diacetylpyridine-bis-4-methoxyaniline, and ImH = Imidazole, have been synthesized and characterized by elemental analysis, FAB mass spectrometry, magnetic susceptibility, X-band electron paramagnetic resonance (EPR), electronic spectroscopy, and cyclic voltammetry. Frozen solution EPR spectra of the complexes have axial features with $g_\parallel > g_\perp > 2.003$ suggesting the presence of a $d_{x^2-y^2}$ ground state. Single crystal X-ray analyses of **1**–**3** reveal the presence of distorted octahedral geometry. All complexes exhibit significant superoxide dismutase activity.

*Keywords*: Copper(II) complexes; X-band EPR; Superoxide dismutase activity

## 1. Introduction

Copper(II) complexes have a wider range of coordination geometries than any other transition metal ions [1]. Recently, tridentate ligands have been extensively used in coordination chemistry [2–7] of copper(II). Interest in these systems is related to the possibility of obtaining low-symmetry five- or six-coordinate complexes, especially if significant steric restrictions are present [8, 9].

Copper complexes have shown anti-inflammatory, antitumor, anticonvulsant, antidiabetic, anticancer, anticarcinogenic, antimutagenic, and radioprotectant activities in animal models of diseased states [10–14]. Oberley and Buettner [15] have observed that cancer cells had less superoxide dismutase (SOD) activity than normal cells. Superoxide ion is toxic to cells; a defense mechanism must have been initiated by nature. All organisms, which use dioxygen and many that have to survive an oxygenated

---

*Corresponding author. Email: rnp64@yahoo.co.uk

environment, contain at least one SOD. The SOD shows biocatalytic activity toward the dismutation of superoxide according to the following mechanism [16]:

$$O_2^- + Cu(II) \longrightarrow O_2 + [Cu^I] \tag{1}$$

$$O_2^- + [Cu^I] + 2H^+ \longrightarrow H_2O_2 + Cu^{II} \tag{2}$$
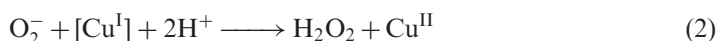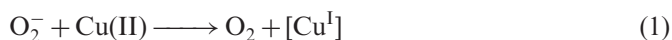
This has led to successful testing of $Cu(II)_2(aspirinate)_4$ and copper(II) salicylates against the growth of solid tumors in implanted mice. Subsequently, several octahedral copper(II) complexes, $[Cu(II)(aspirinate)_2L_2]$, where $L_2$ is pyridine, dimethyl sulphoxide 4-picoline, imidazole, 1-methylimidazole, have been synthesized and SOD activity of these octahedral complexes measured [17]. Various Schiff bases and their metal complexes have been reported [18–21], but the relationship between structures and functions has rarely been investigated. Recently, Han *et al.* [22] studied transition metal (Cu, Zn) complexes with a Schiff base (salicylideneglycine) and 1,10-phenanthroline. We [23–26] have also reported similar work on copper(II) complexes using polyamines and Schiff bases. In this article, we describe the synthesis and characterization of a series of copper(II) complexes using tridentate (PSBP, DAPBMA) and monodentate (ImH) ligands. The crystal structures of these complexes, $[Cu(PSBP)_2](NO_3)(BF_4)$ (**1**), $[Cu(DAPBMA)_2](BF_4)_2$ (**2**), and $[Cu(ImH)_4(NO_3)_2]$ (**3**), are described. The SOD activities have been measured using alkaline DMSO as a source of superoxide radical ($O_2^-$) and nitro blue tetrazolium (NBT) as $O_2^-$ scavenger.

## 2. Experimental

### 2.1. *Materials*

Copper(II) nitrate trihydrate was purchased from S.D. Fine Chemicals, India. All other chemicals used were of synthetic grade and used without purification.

### 2.2. *Synthesis*

The reported complexes were synthesized by the following procedures.

**2.2.1. [Cu(PSBP)₂](NO₃)(BF₄) (1).** To a MeOH solution (10 mL) of $CuNO_3 \cdot 3H_2O$ (1.0 mmol, 0.242 g) a MeOH solution (10 mL) of PSBP (2 mmol, 0.633 g) was added while stirring for 30 min at room temperature. To this reaction mixture, $NH_4BF_4$ (1.0 mmol, 0.105 g) was added and stirred for additional 30 min. After completion of the reaction, dirty green precipitate was formed and collected, washed with methanol and diethyl ether, then dissolved in 1:1 volume of methanol and acetonitrile for recrystallization. The resultant clear solution was left for slow evaporation. After 3–4 days, light yellow crystals were collected which were suitable for X-ray crystallography and washed with MeOH and diethyl ether, dried in air at room temperature, and stored in a $CaCl_2$ desiccator, yield 60%. Anal. Calcd for $C_{38}H_{32}BCuF_4N_9O_5$ (**1**) (%): C, 53.96; H, 3.79; N, 14.91. Found (%): C, 53.93; H, 3.81; N, 14.93. FAB Mass (*m/z*) Calcd: 694. Found: 696.

**2.2.2. [Cu(DAPBMA)$_2$](BF$_4$)$_2$ (2).** A methanolic solution (10 mL) of DAPBMA (2.0 mmol, 0.747 g) was added to a solution of Cu(NO$_3$)$_2 \cdot$ 3H$_2$O (1.0 mmol, 0.242 g) in CH$_3$OH (10 mL) and stirred for 30 min at room temperature. To this reaction mixture was added NH$_4$BF$_4$ (2.0 mmol, 0.210 g) and further stirred for 20 min. After a few days, products suitable for X-ray analysis were collected, washed, air dried, and stored in CaCl$_2$ desiccators. Yield 68%. Anal. Calcd for C$_{46}$H$_{46}$B$_2$CuF$_8$N$_6$O$_4$ (2) (%): C, 56.09; H, 4.67; N, 8.54. Found (%): C, 56.12; H, 4.65; N, 8.56. FAB Mass ($m/z$) Calcd: 810.5. Found: 809.

**2.2.3. [Cu(ImH)$_4$(NO$_3$)$_2$] (3).** To a methanolic solution (10 mL) of Cu(NO$_3$)$_2 \cdot$ 3H$_2$O (1.0 mmol, 0.242 g) was added ImH (4.0 mmol, 0.272 g). The resulting blue solution was stirred for 30 min and allowed to cool and stand for several days; blue crystals of the desired complexes were deposited. Deposited crystals were collected, dried, and stored in CaCl$_2$ desiccators. Yield: 73%. Anal. Calcd for C$_{12}$H$_{16}$CuN$_{10}$O$_6$ (3) (%): C, 31.31; H, 3.48; N, 30.44. Found (%): C, 31.34; H, 3.46; N, 30.45. FAB mass ($m/z$) Calcd: 459.5. Found: 461.

### 2.3. Physical measurements

Elemental analyses were performed on an Elementar Vario EL III Carlo Erba 1108 analyzer. FAB mass spectra were recorded on a JEOL SX 102/DA 6000 mass spectrometer using xenon (6 kV, 10 mA) as the FAB gas. The accelerating voltage was 10 kV and the spectra were recorded at room temperature. UV-Vis spectra were recorded at 25°C on a Shimadzu UV-Vis recording spectrophotometer UV-160 in quartz cells. IR spectra were recorded in KBr on a Perkin-Elmer 783 spectrophotometer from 4000 to 200 cm$^{-1}$. X-band electron paramagnetic resonance (EPR) spectra were recorded with a Varian E-line Century Series spectrometer equipped with a dual cavity and operating at X-band (~9.4 GHz) with 100 kHz modulation frequency. TCNE was used as field marker. The frozen solutions at liquid nitrogen temperature used for EPR spectra were in $3 \times 10^{-3}$ M in DMSO. Varian quartz tubes were used for measuring EPR spectra of polycrystalline samples and frozen solutions. The EPR parameters for copper(II) complexes were determined accurately from a computer simulation program [27]. Magnetic susceptibility measurements were made on a Gouy balance using mercury(II) tetrathiocyanato cobaltate(II) as calibrating agent ($\chi_g = 16.44 \times 10^{-6}$ cgs units). Cyclic voltammetry was carried out with a BAS-100 Epsilon electrochemical analyzer having an electrochemical cell with a three-electrode system. Ag/AgCl was used as a reference electrode, glassy carbon as working electrode, and platinum wire as an auxiliary electrode. A 0.1 M NaClO$_4$ was used as supporting electrolyte and DMSO as solvent. All measurements were carried out at 298 K under nitrogen. The in vitro SOD activity was measured using alkaline DMSO as a source of superoxide radical (O$_2^-$) and NBT chloride as O$_2^-$ scavenger [17, 22]. Molar conductivities of the freshly prepared $2 \times 10^{-3}$ M of DMSO solutions were measured on a Systronics conductivity TDS meter 308.

### 2.4. Crystal structure determination

Crystals suitable for single crystal X-ray analysis for **1**–**3** were grown from slow evaporation of the reaction mixtures at room temperature. The crystals were mounted on a glass fiber and used for data collection. Crystal data were collected on an

Enraf-Nonius MACH$_3$ diffractometer using graphite monochromated Mo-K$\alpha$ radiation ($\lambda = 0.71073$ Å). Crystal orientation, cell refinement and intensity measurements were made using CAD-4PC performing $\Psi$-scan measurements. The structures were solved by direct methods using SHELXS-97 [28] and refined by full-matrix least-square techniques against $F^2$ using SHELXL-97 [29]. All nonhydrogen atoms were refined anisotropically. All hydrogens were geometrically fixed and allowed to refine using a riding model.

## 3. Results and discussion

Octahedral copper(II) complexes were prepared by the following method.

$$Cu^{2+} + A \longrightarrow [Cu(A)_2]X_2 \tag{3}$$

$$Cu^{2+} + B \longrightarrow [Cu(B)_4(X)_2] \tag{4}$$
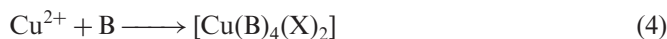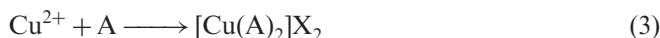
A = PSBP or DAPBMA, X = (NO$_3$)(BF$_4$)/BF$_4$, B = ImH.

Molar conductivity in DMSO shows nonconductor behavior [30] (11 ohm$^{-1}$ cm$^2$ mol$^{-1}$) for **3** and 2 : 1 electrolyte (137 ohm$^{-1}$ cm$^2$ mol$^{-1}$) for **1,** and (149 ohm$^{-1}$ cm$^2$ mol$^{-1}$) for **2**. Room temperature effective magnetic moments $\mu_{\text{eff}}$ of the three complexes are 1.79, 1.81, and 1.82 B.M., respectively, quite close to the values expected for copper(II) complexes [31–33].

### 3.1. *Crystal structure*

The structures of **1**–**3** have been confirmed by a single crystal X-ray study as distorted octahedral geometry around copper(II) by two neutral ligands in complexes **1** and **2**. The coordination geometry $(4 + 2)$ of complex **3** is formed by four ImH and two NO$_3^-$. ORTEP views of these complexes are shown in figures 1–3. Crystallographic data and structure refinement parameters are given in table 1. The relevant bond lengths and angles are listed in tables 2–4. Structures of **1** and **2** are quite similar with octahedral structures consisting of two chemically equivalent neutral tridentate (NNN/NNO) Schiff bases and a copper(II) in discrete monomeric species. The bond distances of the donors of the Schiff base to copper for **1** and **2** are in the range 1.926(5)–2.214(5) Å, close to ~2.0 Å, typical of copper(II) complexes [4, 7, 15].

The copper in **1** and **2** is nested in an axially distorted compressed octahedral N$_6$/N$_4$O$_2$, probably due to Jahn–Teller distortion. In these complexes, neutral tridentate Schiff bases form two fused five-member chelate rings. Ligands are meridional, situated in perpendicular planes in an idealized octahedron. However, the disposition of the ligands deviates noticeably from perpendicularity as indicated by decreased values of the *trans*-angle between the nitrogens N(2)–Cu(1)–N(6) = 171.8(2)° for **1** and N(5)–Cu(1)–N(2) = 176.1(2)° for **2**. A significant difference in interligand *cis* angles is associated with the same Cu–N (py) bond [76.2(2) and 111.1(2)° for the angles involving the Cu(1)–N(5) bond and 89.25(10) and 92.71(18)° for Cu(1)–O(2) bond] for **1** and Cu–N (double bonded) bond [87.12(19) and 76.7(2) for the angles involving Cu(1)–N(1) bond and 106.8(2) and 84.95(19) for the Cu(1)–N(3) bond] for **2**.
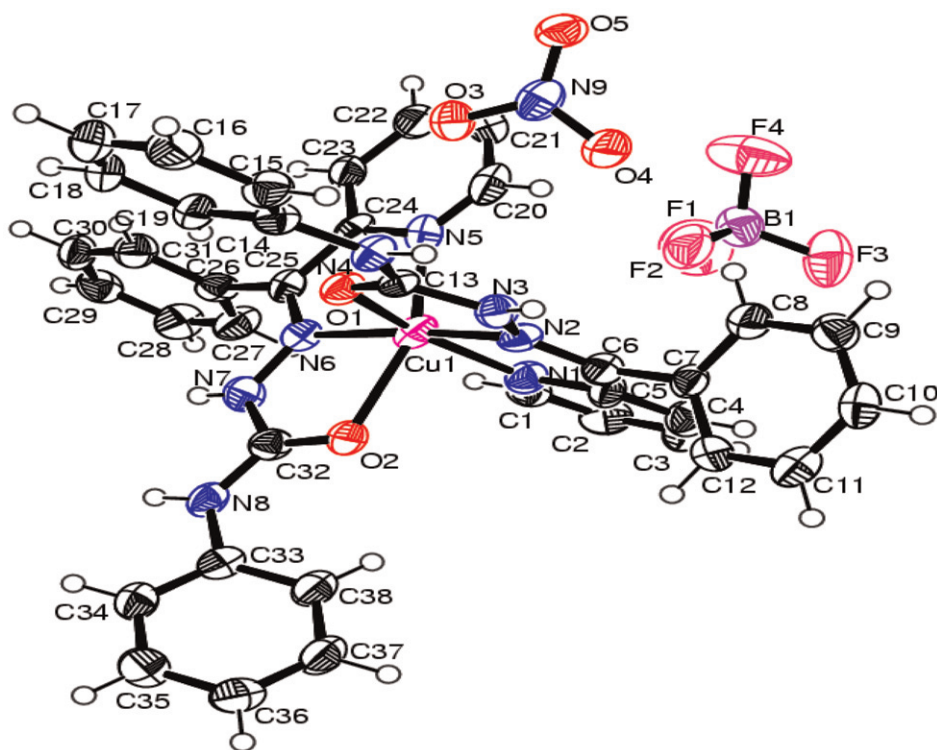
Figure 1. Projection view of **1**.

The Cu–N(py) bond and Cu–O(2) (carboxyl) bonds (2.149(6) and 2.189(5)) occupying equatorial positions are significantly longer than the equatorial Cu–N(1)/ O(1) (py/carboxyl) [2.035(5) and 2.034(4) Å] for **1** and Cu(1)–N bonds (2.216(6) and 2.205(5)) occupying the equatorial positions are significantly longer than the equatorial Cu–N [2.149(5) and 2.167(5)], although the latter are formed by deprotonated groups. This difference is dictated by the bis (chelating) mode of the ligand in which the Cu–N/ O bonds (hydrogen nitrogen ($N_{hydrogen}$) and carbonyl oxygen ($O_{carboxyl}$)) appear to be shared by two five-membered chelate rings. Similar observations are made for complexes having very similar coordination sphere [34].

The NNO/NNN coordination mode defines two five-membered chelate rings whose bite angle constraints are responsible for deviation from linearity of N–Cu–O/N–Cu–N angles. Within these systems, the shortest bonds are those relative to coordination of the $N_{hydrogen}$ or pyridine nitrogen ((Npy) [Cu–N(py) = 1.950(4)–2.017(5) and 2.017(5) Cu– N(py) = 1.926(5)–1.959(5) for both ligands) while the remaining coordination sites are weaker (tables 2 and 3).

The crystal structure of **3** consists of $N_4O_2$ (4 + 2) chromophore in an elongated rhombic octahedral. The four imidazoles are nearly symmetrical in plane with mean Cu–N distance 2.00 Å, with oxygens from $NO_3^-$ occupying the fifth and sixth coordination positions at ~2.54 Å for Cu1–O6 and 2.57 Å for Cu1–O1. The large Cu–O bond distances may be semicoordinated [35, 36].
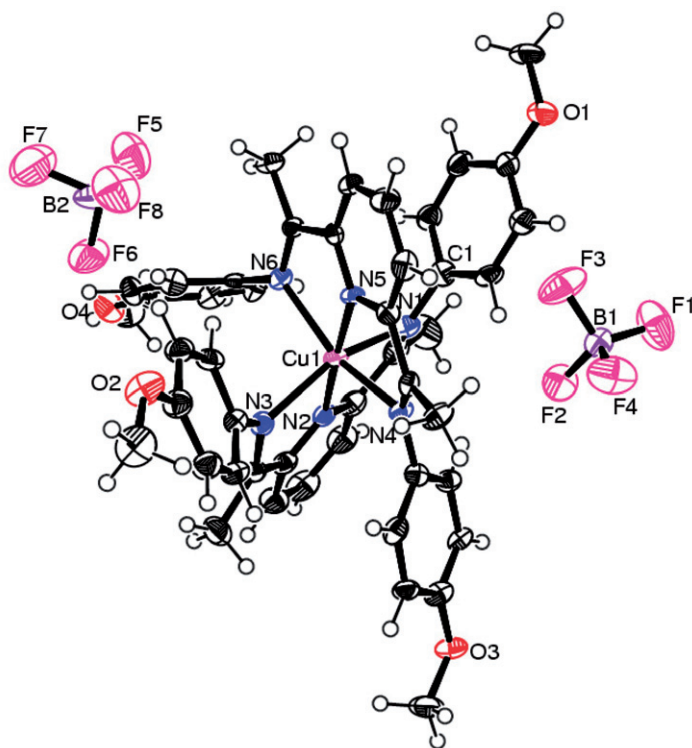
Figure 2. Projection view of **2**.

In **1**, significant hydrogen bonding occurs (figure 4), built from N–H···O and C–H···F (intermolecular hydrogen bonding) and C–H···O (intermolecular hydrogen bonding). The relevant hydrogen bonding distances are given in table 5. The uncoordinated tetrafluoroborate and nitrates play a significant role in the hydrogen bonding, acting as bridges connecting neighboring copper(II) dimeric units. A weak interaction between H(19) of C(19) with O(9) and H(38) of C(38) with O(2) as C–H–F are seen. Similarly, some more weak hydrogen bonding (intermolecular) is seen.

### 3.2. *Electron paramagnetic resonance*

The EPR spectra of polycrystalline samples at 298 K and in solution at 77 K were recorded in the X-band region. Some representative spectra are shown in 'Supplementary material' and EPR parameters are presented in table 6. EPR spectra of **1** and **3** are slightly orthorhombic. Complex **3** exhibits a well-resolved hyperfine structure in the $g_z$ component. Complex **2** exhibits isotropic spectra with $g_{iso} = 2.058$. The three complexes do not show the $\Delta M_s = \pm 2$ signal, indicating absence of copper(II) dimers at 77 K. The frozen solution spectra of the three complexes are axial with $g_\parallel > g_\perp > 2.0$, suggesting the presence of a $d_{x^2-y^2}$ ground state [37, 38]. The geometric
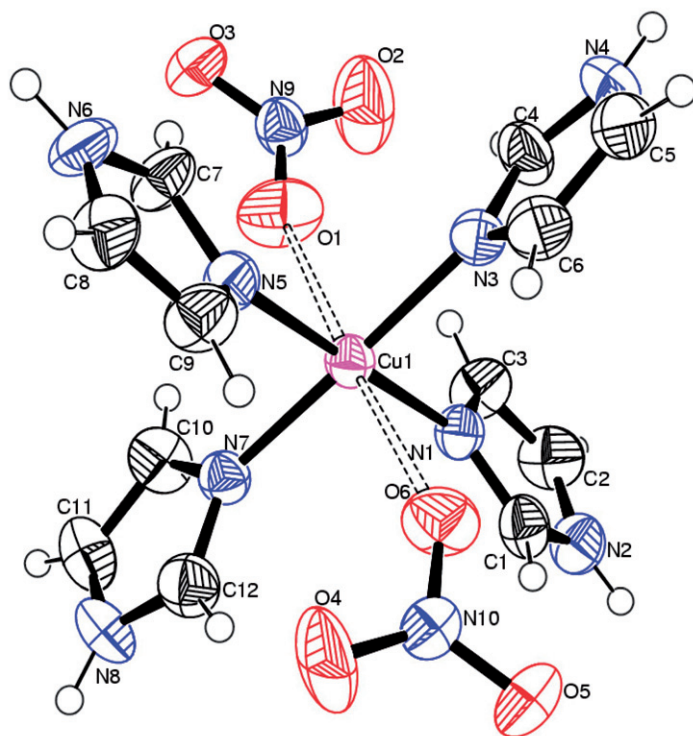
Figure 3.   Projection view of **3**.

Table 1.   Crystal data and structure refinement for **1**–**3**.

| | **1** | **2** | **3** |
|---|---|---|---|
| Empirical formula | $C_{38}H_{32}BCuF_4N_9O_5$ | $C_{46}H_{46}B_2CuF_8N_6O_4$ | $C_{12}H_{16}CuN_{10}O_6$ |
| Formula weight | 845.08 | 984.05 | 459.89 |
| Temperature (K) | 150(2) | 150(2) | 150(2) |
| Wavelength (Å) | 0.71073 | 0.71073 | 0.71073 |
| Crystal system | Monoclinic | Monoclinic | Orthorhombic |
| Space group | $P2_1/n$ | $P2_1/a$ | $Pna21$ |
| Unit cell dimensions (Å, °) | | | |
| $a$ | 13.999(3) | 16.5299(7) | 13.8938(6) |
| $b$ | 15.946(4) | 16.5590(6) | 9.8032(5) |
| $c$ | 16.457(3) | 17.1209(9) | 13.3928(8) |
| $\alpha$ | 90 | 90 | 90 |
| $\beta$ | 96.281(16) | 108.188(5) | 90 |
| $\gamma$ | 90 | 90 | 90 |
| Volume (Å$^3$), $Z$ | 3651.7(13), 4 | 4452.2(3), 4 | 1824.15(16), 4 |
| Calculated density (mg m$^{-3}$) | 1.537 | 1.468 | 1.675 |
| Absorption coefficient (mm$^{-1}$) | 0.678 | 0.576 | 1.254 |
| $F(000)$ | 1732 | 2028 | 940 |
| Crystal size (mm$^3$) | $0.23 \times 0.18 \times 0.16$ | $0.33 \times 0.26 \times 0.21$ | $0.33 \times 0.27 \times 0.22$ |
| Goodness-of-fit on $F^2$ | 0.999 | 1.128 | 0.932 |
| Final $R$ indices [$I > 2\sigma(I)$] | $R_1 = 0.0783$, $wR_2 = 0.1609$ | $R_1 = 0.0923$, $wR_2 = 0.2096$ | $R_1 = 0.0604$, $wR_2 = 0.1033$ |
| $R$ indices (all data) | $R_1 = 0.1579$, $wR_2 = 0.1931$ | $R_1 = 0.1261$, $wR_2 = 0.2298$ | $R_1 = 0.0604$, $wR_2 = 0.1033$ |

Table 2. Selected bond lengths (Å) and angles (°) of **1**.

| | | | |
|---|---|---|---|
| Cu(1)–N(2) | 1.950(4) | N(6)–C(24) | 1.343(6) |
| Cu(1)–N(6) | 2.017(5) | N(6)–C(25) | 1.298(7) |
| Cu(1)–O(1) | 2.084(4) | N(3)–C(13) | 1.380(7) |
| Cu(1)–N(1) | 2.085(5) | N(4)–C(13) | 1.328(8) |
| Cu(1)–O(2) | 2.189(5) | N(4)–C(13) | 1.321(7) |
| Cu(1)–N(5) | 2.149(6) | N(4)–C(14) | 1.423(7) |
| N(1)–C(1) | 1.308(8) | N(6)–N(7) | 1.366(7) |
| N(1)–C(5) | 1.367(7) | N(7)–C(32) | 1.379(7) |
| N(2)–C(6) | 1.287(7) | N(8)–C(32) | 1.340(8) |
| N(2)–N(3) | 1.345(7) | N(8)–C(33) | 1.412(8) |
| N(5)–C(20) | 1.316(9) | | |
| N(2)–Cu(1)–N(6) | 171.8(2) | N(1)–Cu(1)–O(2) | 92.71(18) |
| N(2)–Cu(1)–O(1) | 78.03(17) | N(5)–Cu(1)–O(2) | 151.44(16) |
| N(6)–Cu(1)–O(1) | 97.77(17) | C(6)–N(2)–Cu(1) | 120.3(4) |
| N(2)–Cu(1)–N(1) | 79.23(19) | N(3)–N(2)–Cu(1) | 115.9(4) |
| N(6)–Cu(1)–N(1) | 104.68(19) | C(20)–N(5)–Cu(1) | 127.1(4) |
| O(1)–Cu(1)–N(1) | 157.23(16) | C(24)–N(5)–Cu(1) | 11.9(4) |
| N(2)–Cu(1)–N(5) | 111.2(2) | C(25)–N(6)–Cu(1) | 121.0(5) |
| N(6)–Cu(1)–N(5) | 76.2(2) | N(6)–Cu(1)–N(7) | 117.2(4) |
| O(1)–Cu(1)–N() | 96.51(17) | N(2)–Cu(1)–O(2) | 97.46(18) |
| N(1)–Cu(1)–N(5) | 92.56(19) | N(1)–Cu(1)–O(2) | 92.71(18) |
| N(2)–Cu(1)–N(6) | 171.8(2) | N(5)–Cu(1)–O(2) | 151.44(16) |
| N(2)–Cu(1)–O(1) | 78.03(17) | C(6)–N(2)–Cu(1) | 120.3(4) |
| N(6)–Cu(1)–O(1) | 97.77(17) | N(3)–N(2)–Cu(1) | 115.9(4) |
| N(2)–Cu(1)–N(1) | 79.23(19) | | |

Table 3. Selected bond lengths (Å) and angles (°) of **2**.

| | | | |
|---|---|---|---|
| Cu(1)–N(2) | 1.959(5) | Cu(1)–N(6) | 2.149(5) |
| Cu(1)–N(4) | 2.167(5) | N(3)–C(15) | 1.282(8) |
| Cu(1)–N(1) | 2.216(5) | N(3)–C(17) | 1.420(8) |
| Cu(1)–N(3) | 2.205(5) | N(4)–C(31) | 1.278(8) |
| Cu(1)–N(5) | 1.926(5) | N(4)–C(24) | 1.422(8) |
| N(1)–C(8) | 1.272(9) | N(5)–C(34) | 1.340(8) |
| N(1)–C(1) | 1.415(9) | N(5)–C(38) | 1.344(7) |
| N(2)–C(14) | 1.343(8) | N(6)–C(39) | 1.278(8) |
| N(2)–C(10) | 1.343(8) | N(6)–C(41) | 1.429(8) |
| N(5)–Cu(1)–N(2) | 176.1(2) | N(2)–Cu(1)–N(1) | 76.7(2) |
| N(5)–Cu(1)–N(6) | 78.0(2) | N(6)–Cu(1)–N(1) | 87.12(19) |
| N(2)–Cu(1)–N(6) | 101.6(2) | N(4)–Cu(1)–N(1) | 97.3(2) |
| N(5)–Cu(1)–N(4) | 77.6(2) | N(3)–Cu(1)–N(1) | 153.5(2) |
| N(2)–Cu(1)–N(4) | 102.8(2) | C(8)–N(1)–Cu(1) | 112.1(5) |
| N(6)–Cu(1)–N(4) | 155.6(2) | C(1)–N(1)–Cu(1) | 119.8(4) |
| N(5)–Cu(1)–N(3) | 106.8(2) | C(14)–N(2)–Cu(1) | 119.4(4) |
| N(2)–Cu(1)–N(3) | 77.1(2) | C(10)–N(2)–Cu(1) | 119.5(5) |
| N(6)–Cu(1)–N(3) | 101.73(19) | C(15)–N(3)Cu(1) | 112.3(4) |
| N(4)–Cu(1)–N(3) | 84.95(19) | C(17)–N(3)–Cu(1) | 122.2(4) |
| N(5)–Cu(1)–N(1) | 99.4(2) | C(31)–N(4)–Cu(1) | 112.9(4) |
| C(24)–N(4)–Cu(1) | 118.9(4) | C(39)–N(6)–Cu(1) | 112.5(4) |
| C(34)–N(5)–Cu(1) | 119.3(4) | C(41)–N(6)–Cu(1) | 125.3(4) |
| C(38)–N(5)–Cu(1) | 118.7(4) | | |

parameter *G* is a measure of the exchange interaction. The values of *G* for **1**–**3** are in the range 3.5–4.0, indicating little interaction in polycrystalline state [39, 40].

The EPR parameters and d–d transition energies were used to evaluate the bonding parameter $\alpha^2$, $\beta^2$, and $\gamma^2$, a measure of the covalency of the in-plane $\sigma$ bonding and the in-plane $\pi$- and out-of-plane $\pi$ bonding, respectively. Significant information about the

Table 4.   Selected bond lengths (Å) and angles (°) of **3**.

| | | | |
|---|---|---|---|
| Cu(1)–N(3) | 2.000(4) | N(2)–C(1) | 1.333(10) |
| Cu(1)–N(5) | 1.999(5) | N(3)–C(4) | 1.318(9) |
| Cu(1)–N(7) | 2.005(4) | O(2)–N(9) | 1.199(8) |
| Cu(1)–O(6) | 2.541 | N(5)–C(7) | 1.314(8) |
| Cu(1)–O(1) | 2.571 | N(5)–C(9) | 1.392(8) |
| Cu(1)–N(1) | 2.007(5) | N(6)–C(7) | 1.312(11) |
| O(1)–N(9) | 1.197(9) | N(6)–C(8) | 1.374(11) |
| O(3)–N(9) | 1.244(8) | N(7)–C(12) | 1.306(8) |
| O(4)–N(10) | 1.240(8) | N(7)–C(10) | 1.399(8) |
| O(5)–N(10) | 1.221(7) | N(8)–C(11) | 1.318(9) |
| O(6)–N(10) | 1.245(8) | N(8)–C(12) | 1.329(7) |
| N(1)–C(1) | 1.294(8) | N(4)–C(4) | 1.313(7) |
| N(1)–C(3) | 1.373(8) | N(4)–C(5) | 1.370(10) |
| N(2)–C(2) | 1.335(11) | | |
| N(3)–Cu(1)–N(5) | 89.5(2) | N(3)–Cu(1)–N(7) | 178.72(16) |
| N(5)–Cu(1)–N(7) | 89.9(2) | C(9)–N(5)–Cu(1) | 128.5(4) |
| C(3)–N(1)–Cu(1) | 127.6(4) | C(12)–N(7)–Cu(1) | 129.2(4) |
| C(6)–N(3)–Cu(1) | 125.7(5) | C(4)–N(3)–Cu(1) | 127.3(5) |
| C(1)–N(1)–Cu(1) | 126.9(5) | N(7)–Cu(1)–N(1) | 90.6(2) |
| N(5)–Cu(1)–N(1) | 179.3(2) | C(10)–N(7)–Cu(1) | 125.7(4) |
| | | N(3)–Cu(1)–N(1) | 90.0(2) |
| | | C(7)–N(5)–Cu(1) | 126.2(5) |
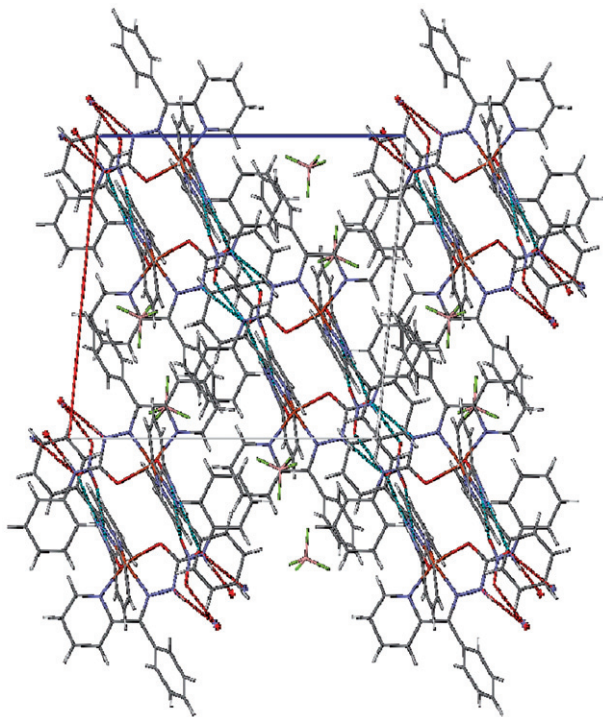


Figure 4.   Unit cell view of **1**.

Table 5.  Hydrogen bonding interactions of **1** (Å and °).

| D–H$\cdots$A | D–H (Å) | H$\cdots$A (Å) | D$\cdots$A (Å) | $\angle$D–H$\cdots$A (°) |
|---|---|---|---|---|
| N(7)–H(3N)$\cdots$O(5) | 0.77(6) | 2.21(6) | 2.962(7) | 165(6) |
| N(4)–H(4)$\cdots$O(4) | 0.88 | 2.07 | 2.843(7) | 146 |
| N(3)–H(7N)$\cdots$O(5) | 0.82(5) | 2.13(5) | 2.931(7) | 167(5) |
| N(8)–H(8)$\cdots$O(3) | 0.88 | 2.01 | 2.824(6) | 154 |
| C(12)–H(12)$\cdots$F(3) | 0.95 | 2.41 | 3.234(8) | 145 |
| C(16)–H(16)$\cdots$F(3) | 0.95 | 2.53 | 3.321(8) | 140 |
| Intra C(19)–H(19)$\cdots$O(1) | 0.95 | 2.26 | 2.877(7) | 122 |
| C(20)–H(20)$\cdots$F(2) | 0.95 | 2.31 | 3.043(7) | 133 |
| C(28)–H(28)$\cdots$F(3) | 0.95 | 2.53 | 3.172(7) | 125 |
| C(34)–H(34)$\cdots$O(3) | 0.95 | 2.49 | 3.253(8) | 137 |
| Intra C(38)–H(38)$\cdots$O(2) | 0.95 | 2.31 | 2.838(9) | 114 |

nature of bonding in the copper(II) complexes can be derived from the magnitude of $K_{\parallel}$ and $K_{\perp}$. In case of pure $\sigma$ bonding, $K_{\parallel} \sim K_{\perp} \sim 0.77$ whereas $K_{\parallel} < K_{\perp}$ implies considerable in-plane bonding, while for out-of-plane bonding $K_{\parallel} > K_{\perp}$. In the present copper(II) complexes, $K_{\parallel} < K_{\perp}$ indicating significant in-plane bonding. The values of $\alpha^2$, $\beta^2$, and $\gamma^2$ are consistent with strong in-plane $\sigma$ and in-plane $\pi$ bonding. The computed value (table 6) of $\alpha^2$ and $\beta^2$, compared with other copper(II) complexes, are ionic in nature [41]. The empirical factor $f = g_{\parallel}/A_{\parallel}$ (cm$^{-1}$) is an index of tetragonal distortions and its value may vary from 105 to 135 for small to extreme distortions in octahedral complexes, depending on the nature of the coordinated atoms [42]. The $f$ values of these complexes are in the range 134–151, indicating significant distortion from planarity.

### 3.3. *Electronic absorption spectra*

Complexes **1** and **3** show a broad nonsymmetric band with absorption maximum at $\sim$650 nm and at $\sim$400 nm (500 M$^{-1}$ cm$^{-1}$) assigned as LMCT. Such observations [43–45] are consistent with octahedral copper(II) complexes. The electronic spectrum of **2** in DMSO consists of a featureless band at 400 nm, typical of a distorted *trans*-Cu$^{II}$N6 chromophore [46]. The complex also exhibits absorption at 300 nm assignable to LMCT transition [47]. All these values are far from that of aqueous CuCl$_2$ at 819 nm, indicating the complexes are not dissociated in solution.

### 3.4. *IR spectra*

A strong band at 270–295 cm$^{-1}$ is consistent with the $\nu$(Cu–N$_{py}$) [48]. Valence vibration of N–H of the secondary acyclic amine can be observed around 1620 cm$^{-1}$. Characteristic IR vibrations of **1** are: $\nu$(Cu–N$_{azo}$) = 460 cm$^{-1}$, $\nu$(Cu–N$_{py}$) = 276 cm$^{-1}$, $\nu$(C=O) = 1670 cm$^{-1}$, $\nu$(N–N) = 1125 cm$^{-1}$, $\nu$(C=N) = 1550 cm$^{-1}$, $\nu$(C–N$_{ali/aro}$) = 1150 cm$^{-1}$/1300 cm$^{-1}$, $\nu$(C=N) = 550 cm$^{-1}$, $\nu$(N–H) $\approx$ 1600 cm$^{-1}$. The $\nu$(C=N) band of the ligand at 1621 cm$^{-1}$ is shifted to lower energies (1586–1595 cm$^{-1}$) in **1** indicating coordination *via* the azomethine. This is confirmed by bands in the range 459–461 cm$^1$, which have been assigned to $\nu$(Cu–N$_{azo}$). Based on the above spectral evidence,

Table 6. EPR spectral parameters of **1**–**3**.

| | 1 | 2 | 3 |
|---|---|---|---|
| **Polycrystalline state (298 K)** | | | |
| $g_1$ | 2.15 | | 2.15 |
| $g_2$ | 2.07 | | 2.05 |
| $g_3$ | 2.01 | | 2.02 |
| $g_{iso}/g_{ave}$ | 2.15 | 2.06 | 2.25 |
| **DMSO (77 K)** | | | |
| $g_{\parallel}$ | 2.27 | 2.25 | 2.21 |
| $g_{\perp}$ | 2.07 | 2.07 | 2.06 |
| $A_{\parallel}$ (G) | 150 | 160 | 165 |
| $G$ | 4.06 | 3.5 | 3.61 |
| $\alpha^2$ | 0.72 | 0.74 | 0.70 |
| $\beta^2$ | 0.94 | 0.76 | 0.96 |
| $\gamma^2$ | 0.96 | 0.72 | 0.99 |
| $K_{\parallel}$ | 0.77 | 0.97 | 0.67 |
| $K_{\perp}$ | 0.75 | 1.02 | 0.70 |
| $f$ (cm) | 151 | 140 | 134 |

the ligand in **1** is tridenatate coordinating *via* the azomethine nitrogen and carboxylate oxygen. Similarly, the characteristic IR vibrations of **2** and **3** can be represented as $\nu(C=N) = 1540\,cm^{-1}$, $\nu(C=O_{methoxy}) = 1215\,cm^{-1}$ and $\nu(C=N) = 1535\,cm^{-1}$, $\nu(Cu–ONO_2) = 272\,cm^{-1}$ for **2** and **3**, respectively. The broadband of **3** at $1386\,cm^{-1}$ and the weak band at $1753\,cm^{-1}$ are due to unidentate $NO_3^-$ [49].

### 3.5. *Electrochemical studies*

Electroactivity of the complexes was studied in DMSO with $0.1\,M$ NaClO$_4$ as supporting electrolyte using cyclic voltammetry at a platinum working electrode. A representative voltammogram is shown in 'Supplementary material' and redox potential values are given in table 7. The redox processes assigned as Cu(II)/Cu(I) couples are irreversible. The voltammograms of the complexes consist of two well-separated peaks, one cathodic potential ($E_{pc}$) and one anodic potential ($E_{pa}$). In these complexes, reduction values were observed at more negative potential. The one electron stoichiometry of couple was confirmed by comparison of the current with that of a known [50] Cu$^I$–Cu$^{II}$ couple. The peak current ratio $I_{pa}/I_{pc}$ is less than unity, showing that the electron transfer reaction is followed by a chemical reaction (EC mechanism) [51, 52].

### 3.6. *Superoxide dismutase activity*

SOD mimetic activities of **1**–**3** were measured with an indirect method in which alkaline DMSO served as the source for superoxide radicals. SOD values (IC$_{50}$) are in the range $30 \pm 5\,\mu$M. The observed (IC$_{50}$) values of the present complexes are comparable (table 8) to reported values [17, 22, 24]. SOD activities of copper(II) complexes are in the order **3** > **2** ≈ **1**. From this trend, it appears that inclusion of nitrogen donors reduces the SOD activity.

Table 7. Cyclic voltammetric data for 1 mM solution of **1–3** in DMSO containing 0.1 M NaClO$_4$ as supporting electrolytes.

| Scan rate (mV s$^{-1}$) | $E_{pc}$ (mV) | $I_{pc}$ (µA) | $E_{pa}$ (mV) | $I_{pa}$ (µA) | $\Delta E_p$ (mV) | $E^\circ$ (mV) | $I_{pa}/I_{pc}$ (µA) |
|---|---|---|---|---|---|---|---|
| **1** | | | | | | | |
| 100 | −473 | 10.53 | −259 | 5.85 | 214 | −366 | 0.57 |
| 200 | −520 | 14.75 | −212 | 9.12 | 308 | −366 | 0.62 |
| **2** | | | | | | | |
| 100 | −513 | 1.72 | −323 | 1.21 | 190 | −418 | 0.72 |
| 200 | −529 | 7.98 | −311 | 5.37 | 218 | −420 | 0.67 |
| **3** | | | | | | | |
| 100 | −396 | 2.39 | 78 | 0.92 | 474 | −159 | 0.38 |
| 200 | −410 | 3.42 | 90 | 1.38 | 500 | −160 | 0.40 |

$\Delta E_p = E_{pa} - E_{pc}$; $E^\circ = (E_{pa} + E_{pc})/2$.

Table 8. SOD activity of copper(II) complexes by NBT method.

| Complex | Amount required for unit SOD activity (µM) | Reference |
|---|---|---|
| Cu(II)(aspirinate)$_2$(DMSO)$_2$ | >400 | [17] |
| Cu(II)(aspirinate)$_2$(ImH)$_2$ | 160 | [17] |
| Cu(II)(aspirinate)$_2$(4-pic)$_2$ | 100 | [17] |
| Cu(II)(aspirinate)$_2$(1-Meim)$_2$ | 38 | [17] |
| Cu(II)(aspirinate)$_2$(py)$_2$ | 13 | [17] |
| Cu(II)(aspirinate)$_2$(salicylate)$_2$ | 44 | [17] |
| SOD | 0.04 | [17] |
| [Cu(SAA)(H$_2$O)] | 63 | [22] |
| [Cu(SAA)(MeImH)] | 35 | [22] |
| [Cu(SAA)(EtImH)] | 43 | [22] |
| [Cu(SAA)(BenzImH)] | 50 | [22] |
| [Cu(SAA)(MebenzImH)] | 52 | [22] |
| [Cu(SAA)(ImH)] | 30 | [24] |
| [Cu(SAA)(bipy)] | 56 | [24] |
| [Cu(SAA)(phen)] | 50 | [24] |
| [Zn(salgly)(phen)H$_2$O] | 6.15 | [26] |
| [Cu(salgly)(phen)H$_2$O] | 0.79 | [26] |
| [(PSBP)$_2$](NO$_3$)(BF$_4$)] | 35 | This work |
| [Cu(DAPBMA)$_2$](BF$_4$)$_2$] | 34 | This work |
| [Cu(ImH)(NO$_3$)$_2$] | 25 | This work |

## 4. Conclusion

[Cu(PSBP)$_2$](NO$_3$)(BF$_4$) (**1**), [Cu(DAPBMA)$_2$](BF$_4$)$_2$ (**2**), and [Cu(ImH)$_4$(NO$_3$)$_2$] (**3**) are synthesized, characterized with tridentate Schiff bases, and structurally characterized by single crystal X-ray analysis. The EPR spectra of the complexes show axial features. The SOD activities were measured. Competition with NBT toward superoxide shows better for **3**. Complex **3** having similar geometry to that of native SOD may be considered an analogue, but is less active than the native enzyme (SOD).

## Supplementary material

CCDC 698349, 698350, and 698351 contain the supplementary crystallographic data for **1**–**3**. These data can be obtained free of charge *via* http://www.ccdc.cam.ac.uk/conts/retrieving.html, or from the Cambridge Crystallographic Data Centre, 12 Union Road, Cambridge CB2 1EZ, UK, Fax: +44-1223-336033, Email: deposit@ccdc.cam.ac.uk.

## Acknowledgments

## References

[1] B.J. Hathaway. *Struct. Bond. (Berlin)*, **57**, 55 (1984).
[2] J.V. Folgado, W. Henke, R. Allmann, H. Stratermeier, D. Beltran-Porter, T. Rojo, D. Reinen. *Inorg. Chem.*, **29**, 2035 (1990).
[3] J.G. Lozano, L. Soto, J. Vicente Folgado, E. Escriva. *Polyhedron*, **15**, 4003 (1996).
[4] A. Bacchi, G. Pelizzi, D. Jeremic, D. Sladic, M. Gruden-Pavlivic, K. Andjelkovic. *Transition Met. Chem.*, **28**, 935 (2003).
[5] M.J. Young, D. Wahnun, R.C. Hynes, J. Chin. *J. Am. Chem. Soc.*, **117**, 9441 (1995).
[6] A. Sreekanth, M.R.P. Kurup. *Polyhedron*, **22**, 3321 (2003).
[7] A.T. Chaviara, P.J. Cox, K.H. Repana, A.A. Pantazoki, K.J. Papazisis, A.H. Kortsaris, D.A. Kyriakidis, G.S. Nikolov, C.A. Bolos. *J. Inorg. Biochem.*, **99**, 467 (2005).
[8] J. Fergusson. *Prog. Inorg. Chem.*, **12**, 159 (1970).
[9] J.R. Wasson. *Spectrosc. Lett.*, **9**, 95 (1976).
[10] J.R.G. Sorenson. In *Metal Ions in Biological Systems*, H. Sigel (Ed.), Vol. 14, p. 124, Marcel Dekker, New York (1982).
[11] J.R.G. Sorenson, V. Kishore, A. Pezeshk, L.W. Oberley, S.W.C. Leuthauser. *Inorg. Chim. Acta*, **91**, 285 (1984).
[12] J.R.G. Sorenson. *Chem. Ber.*, **16**, 1110 (1984).
[13] R.K. Crouch, T.W. Kensler, L.A. Oberlay, J.R.G. Sorenson. In *Biological and Inorganic Copper Chemistry*, K.D. Karlin, J. Zubieta (Eds), p. 139, Adenine, New York (1986).
[14] J.R.G. Sorenson. *Chem. Ber.*, **21**, 169 (1989).
[15] L.W. Oberley, G.R. Buettner. *Cancer Res.*, **39**, 1141 (1979).
[16] I. Fridovich. *Annu. Rev. Biochem.*, **614**, 147 (1975).
[17] R.G. Bhirud, T.S. Shrivastava. *Inorg. Chim. Acta*, **173**, 121 (1990).
[18] C.P. Horwitz, S.E. Creager, R.W. Murray. *Inorg. Chem.*, **29**, 1006 (1990).
[19] A.S. Al-Shihri. *Spectrochim. Acta, Part A*, **60**, 1189 (2004).
[20] M. Yuan, F. Zhao, W. Zhang, Z.M. Wang, S. Gao. *Inorg. Chem.*, **46**, 11235 (2007).
[21] B.R. Manzano, F.A. Jalón, I.M. Ortiz, M.L. Soriano, F. Gómez de la Torre, J. Elguero, M.A. Maestro, K. Mereiter, T.D.W. Claridge. *Inorg. Chem.*, **47**, 413 (2008).
[22] J. Han, Y. Xing, C. Wang, P. Hou, F. Bai, X. Zeng, X. Zhang, M. Ge. *J. Coord. Chem.*, **62**, 745 (2009).
[23] R.N. Patel, N. Singh, K.K. Shukla, U.K. Chauhan, J. Niclos-Gutierrez, A. Castineiras. *Inorg. Chim. Acta*, **357**, 2469 (2004).
[24] R.N. Patel, N. Singh, V.L.N. Gundla. *Polyhedron*, **25**, 3312 (2006).
[25] R.N. Patel, V.L.N. Gundla, D.K. Patel. *Polyhedron*, **27**, 1054 (2008).

[26] R.N. Patel, V.L.N. Gundla, D.K. Patel. *Indian J. Chem.*, **47A**, 353 (2008).
[27] G. Giugliarelli, S. Cannistraro. *Nuovo Cimento*, **4D**, 194 (1984).
[28] G.M. Sheldrick. *Acta Crystallogr., Sect. A*, **46**, 467 (1990).
[29] G.M. Sheldrick. *SHELXL-97, Program for the Refinement of Crystal Structures*, University of Gottingen, Gottingen, Germany (1997).
[30] W.J. Geary. *Coord. Chem. Rev.*, **1**, 81 (1971).
[31] K. Skorda, S.P. Perlepes, C.P. Raptopoulou, R. Keuters, T. Terzis, J.C. Plakatouras. *Transition Met. Chem.*, **24**, 541 (1999).
[32] R.N. Patel, N. Singh, K.K. Shukla, V.L.N. Gundla, U.K. Chouhan. *Spectrochim. Acta, Part A*, **63**, 21 (2006).
[33] R.N. Patel, N. Singh, K.K. Shukla, V.L.N. Gundla. *Indian J. Chem.*, **45A**, 614 (2006).
[34] A.K. Patra, R. Mukherjee. *Inorg. Chem.*, **38**, 1388 (1999).
[35] B.J. Hathaway. In *Comprehensive Coordination Chemistry*, G. Wilkinson (Ed.), Vol. 5, p. 674, Pergamon Press, Oxford (1985).
[36] B.J. Foley, D. Kennefick, D. Phelan, S. Tyagi, B.J. Hathaway. *J. Chem. Soc., Dalton Trans.*, 2333 (1983).
[37] G. Wilkinson, R.G. Gillard, J.A. McCleverty. *Comprehensive Coordination Chemistry*, **5**, 674 (1987).
[38] A.W. Addison. In *Copper Coordination Chemistry: Biochemical and Inorganic Perspectives*, K.D. Karlin, J. Zubieta (Eds), p. 109, Adenine, Guilderland, New York (1983).
[39] R.J. Rudley, B.J. Hathaway. *J. Chem. Soc.*, 1725 (1970).
[40] B.J. Hathaway, D.E. Billing. *Coord. Chem. Rev.*, **5**, 143 (1970).
[41] B.G. Malmstrom, T. Vanngard. *J. Mol. Biol.*, **2**, 118 (1960).
[42] R. Pogni, M.C. Bartoo, A. Diaz, R. Basosi. *J. Inorg. Biochem.*, **79**, 333 (2000).
[43] G. Wilkinson, R.D. Gillard, J.A. McCleverty. *Comprehensive Coordination Chemistry*, **5**, p. 674, (1994).
[44] A.B.P. Lever, *Inorganic Electronic Spectroscopy*, p. 359, Elsevier, Amsterdam (1968).
[45] A. Pramanik, S. Abbina, G. Das. *Polyhedron*, **26**, 5225 (2007).
[46] A.B.P. Lever. *Inorganic Electronic Spectroscopy*, 2nd Edn, p. 554, Elsevier, Amsterdam (1984).
[47] D. Harrison, B.J. Hathaway. *Acta Crystallogr., Sect. B*, **35**, 2910 (1979).
[48] R.J. Clark, C.S. Williams. *Inorg. Chem.*, **4**, 300 (1965).
[49] K. Nakamoto. *Infrared and Raman Spectra of Inorganic and Co-ordination Compounds*, 4th Edn, p. 228, Wiley, New York (1986).
[50] J. Dindo, V. Roy, G. Mostafa, T.H. Li, A. Usman, I.A. Razak, S. Chantrapromma, H.K. Fun, C. Sinha. *Polyhedron*, **22**, 247 (2003).
[51] D.H. Evans. *Chem. Rev.*, **90**, 739 (1990).
[52] S. Parveen, F. Arjmand. *Indian J. Chem.*, **44A**, 1151 (2005).